Three-Nucleon Clusters in Nuclear Matter*

R. RAJARAMAN
Laboratory of Nuclear Studies, Cornell University, Ithaca, New York
(Received 27 June 1962)

The effect of three-body clusters on the binding energy of nuclear matter is studied. An attempt is made to treat all such clusters of the third order as self-energy diagrams and to include their effect into the single-particle energies, thereby improving the convergence of the Goldstone expansion considerably. For this purpose, an expression for off-diagonal reaction matrix elements is derived. One of the consequences of this procedure is that, to a good approximation, the contribution of all the third-order diagrams together is equal to that arising from just the even "P" states of the simplest of these diagrams. Many of the arguments and approximations used are based on the previous paper of this issue by Bethe *et al.*

I. INTRODUCTION

THE Goldstone[1] linked-cluster expansion for the binding energy of nuclear matter is derived using a total Hamiltonian

$$H=H_0+H_1,$$

where

$$H_0=\sum_i(T_i+U_i),$$

$$H_1=\sum_{i<j} v_{ij}-\sum_i U_i,$$

v_{ij} being the two-particle potential between the pair ij, and U_i being the single-particle self-consistent potential of the ith nucleon.

With the help of the Brueckner reaction matrix

$$G=v-v(H_0-E_0)^{-1}QG, \tag{1}$$

where Q=operator projecting onto states above the Fermi sea and E_0=unperturbed energy of the filled Fermi sea, we can condense these diagrams into those involving only G or U interactions. It was shown[2] that the convergence of the resulting series could be considerably improved by adopting a suitable choice of the single-particle energies U_i. Such convergence is clearly desirable, as it renders the use of just the first-order diagrams to determine the binding energy more exact. For a proper choice of U_i, the diagrams involving "U" interactions should cancel as much as possible of the other diagrams. In effect, this corresponds to including the effect of higher order terms into the first-order diagrams.

The most recent, and perhaps the best such choice is made by the recent work of Bethe, Brandow, and Petschek.[3,4] Their "reference spectrum" for particle energies is so derived that the diagrams in Figs. 1(a), 1(b), and 1(c) together vanish on the average. The reason for their picking Fig. 1(b) and Fig. 1(c) is that among the third-order diagrams (which would provide the largest correction to Brueckner's first-order approximation to the binding energy, there being no second-order diagrams), these are the only ones that look like self-energy diagrams. In other words, the interaction G_2 with the hole "n," can be treated as a self-energy insertion into the energy of particle "b."

Thus, BBP evaluate the middle interaction G_2 in Fig. 1(b) along with its exchange in Fig. 1(c), sum over the hole "n," average over holes l and m and use the result as $U(b)$ in a self consistent manner. This essentially gets rid of Figs. 1(b) and 1(c) with the help of Fig. 1(a), and also Figs. 1(b′) and (1c′) with the help of 1(a′).

The purpose of this paper is to point out the importance of the other third-order diagrams.[5] These can

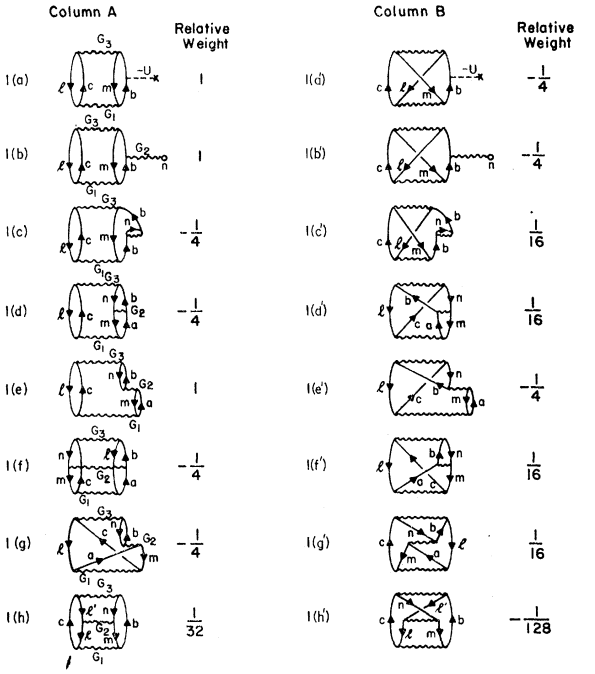

FIG. 1. Third-order diagrams with relative weights as described in Secs. 3 and 4. The diagrams in each column are made to cancel one another by the proper choice of $U(b)$.

* Supported in part by the joint program of the Office of Naval Research and the U. S. Atomic Energy Commission.

[1] J. Goldstone, Proc. Roy. Soc. (London) **A239**, 267 (1957)

[2] K. A. Brueckner and D. T. Goldman, Phys. Rev. **117**, 207 (1960).

[3] H. A. Bethe, B. H. Brandow, and A. G. Petschek, preceding article [Phys. Rev. **129**, 225 (1963)].

[4] From here on referred to as BBP.

[5] One of these graphs was considered by H. S. Köhler, Ann. Phys. (New York) **12**, 444 (1961).

be shown to be comparable in magnitude to the "bubble diagram" of Fig. 1(b), and consequently, deserve to be considered in the same degree of approximation as the latter. It will be shown that, though some of these diagrams are strictly three-nucleon clusters, yet all of them can be treated as self-energy inserts into the particle energies, a privilege that is normally accorded only to Figs. 1(b) and 1(c). Since the BBP work shows that the bubble diagram contributes as much as 4–5 MeV to the binding energy, which is itself only about 15 MeV, one can see that neglecting these other diagrams, which are of comparable size, is quite unjustified. If one were to include their effect into the single-particle energies, as will be done below, then essentially all third-order diagrams are eliminated.

The most important difference between the bubble diagram and the other third-order ones is that while the bubble interaction is diagonal, the latter have off-diagonal interactions in the middle [Figs. 1(c)–1(h)]. Thus we need first to derive an expression for the off-diagonal reaction matrix under the BBP reference spectrum conditions, and study its behavior as compared to the diagonal term. An evaluation of this off-diagonal term is of some value in itself, as it paves a way towards the possible estimation of higher order terms.

II. OFF-DIAGONAL REACTION MATRIX

The reaction matrix in the reference spectrum approximation is defined by

$$G=v-v(H_0-E_0)^{-1}G.$$

The neglect of the Pauli operator Q, as compared to Eq. (1), is justified by BBP. This leads to

$$\langle\phi|\,(H_0-E_0)^{-1}G|\phi_0\rangle=\langle\phi|\phi_0-\psi_0\rangle =\langle\phi|\zeta_0\rangle,$$

where $|\psi_0\rangle$ is the "two-particle wave function" defined by

$$|\psi_0\rangle=[1-(H_0-E_0)^{-1}v +(H_0-E_0)^{-1}v(H_0-E_0)^{-1}v\cdots]|\phi_0\rangle. \quad (2)$$

We are essentially doing a two-body problem with a modified energy spectrum. The problem can be separated into center-of-mass and relative coordinates, the former leading as usual to momentum conservation. We therefore concern ourselves with the relative coordinate problem. In the spirit of the reference spectrum it is assumed that H_0-E_0 can be written in relative coordinates as $-(\hbar^2/Mm^*)(\nabla^2-\gamma^2)$, where γ^2 is a positive number. The fact that the interaction is off the energy shell makes γ^2 more positive.

For simplicity, from here on we will consider all wave functions as contained in a cube of unit volume. We will also suppress the factor $\hbar^2M^{-1}$.

Let $\phi=e^{i\mathbf{k}\cdot\mathbf{r}}$ and $\phi_0=e^{i\mathbf{k}_0\cdot\mathbf{r}}$. From (2) it can be seen that $\zeta_0=\phi_0-\psi_0$ obeys

$$(\nabla^2-\gamma^2)\zeta_0=-m^*v(\phi_0-\zeta_0);$$

ϕ obeys

$$(\nabla^2+k^2)\phi=0. \quad (3)$$

In order to illustrate the behavior of our nondiagonal element as compared to the diagonal ones, we will use the following simple potential:

$$v=\infty \quad \text{for} \quad r<c,$$
$$v=0 \quad \text{for} \quad r>c.$$

Qualitative conclusions analogous to the ones we will derive, hold also for more realistic potentials.

Inside this "hard core," i.e., for $r<c$, we have $\zeta_0=\phi_0=e^{i\mathbf{k}_0\cdot\mathbf{r}}$. The contribution to $\langle\phi|\zeta_0\rangle$ from inside the core is, then,

$$2\pi\int_0^\pi d\theta\sin\theta\int_0^c dr\,r^2e^{-i(\mathbf{k}-\mathbf{k}_0)\cdot\mathbf{r}}=4\pi\{[(qc)^2/q^3]j_1(qc)\}, \quad (4)$$

where $\mathbf{q}=\mathbf{k}-\mathbf{k}_0$. To evaluate the contribution to $\langle\phi|\zeta_0\rangle$ from outside the core, we expand

$$\zeta_0=(k_0r)^{-1}\textstyle\sum_l i^l(2l+1)P_l(\hat{k}_0\cdot\hat{r})\chi_l(k_0r),$$
$$\phi=(kr)^{-1}\textstyle\sum_s i^s(2s+1)P_s(\hat{k}\cdot\hat{r})\mathcal{J}_s(kr),$$

where $\hat{k}_0=\mathbf{k}_0/k_0$, $\hat{r}=\mathbf{r}/r$, and $\hat{k}=\mathbf{k}/k$. Therefore,

$$\int\phi^*\zeta_0d\tau=(kk_0)^{-1}\textstyle\sum_l(2l+1)\sum_s(2s+1) \times\displaystyle\int\frac{d\tau}{r^2}P_l(\hat{k}_0\cdot\hat{r})P_s(\hat{k}\cdot\hat{r})\chi_l(k_0r)\mathcal{J}_s(kr)(i)^{l-s}.$$

Using

$$P_l(\hat{k}_0\cdot\hat{r})=P_l(\hat{k}\cdot\hat{r})P_l(\hat{k}\cdot\hat{k}_0) +\sum_{m=1}^{l}(-1)^m\frac{(l-m)!}{(l+m)!}P_l^m(\hat{k}\cdot\hat{r})P_l^m(\hat{k}\cdot\hat{k}_0)\cos m\phi,$$

we get

$$\int_{r>c}\phi^*\zeta_0d\tau=\frac{4\pi}{kk_0}\textstyle\sum_l(2l+1)P_l(\hat{k}\cdot\hat{k}_0) \times\displaystyle\int_c^\infty\chi_l(k_0r)\mathcal{J}_l(kr)dr. \quad (5)$$

Equations (5) and (4) together give the total contribution to $\langle\phi|\zeta_0\rangle$. Therefore, once we evaluate (5), then we can find the off-diagonal element,

$$\langle\phi|G|\phi_0\rangle=\langle\phi|\,(H_0-E_0)^{-1}G|\phi_0\rangle(k^2+\gamma^2)/m^* =[(k^2+\gamma^2)/m^*]\langle\phi|\zeta_0\rangle.$$

To find the value of the expression in (5), we proceed as follows: Equations (3) reduce to

$$[d^2/dr^2-\gamma^2-l(l+1)/r^2]\chi_l(k_0r) =-m^*v[\mathcal{J}_l(k_0r)-\chi_l(k_0r)]. \quad (6)$$

From (6) it can be proved, as described in Sec. V of BBP, that

$$\int_c^\infty dr\,\chi_l(k_0r)\mathcal{J}_l(kr)$$
$$=(k^2+\gamma^2)^{-1}\Big\{\mathcal{J}_l(k_0c)[\mathcal{J}_l'(kc)-H_l'(c)]$$
$$+\int_c^\infty[\mathcal{J}_l(kr)-H_l(r)]m^*v[\mathcal{J}_l(k_0r)-\chi_l(k_0r)]dr\Big\},$$

where all differentiations are with respect to r. H_l obeys

$$[d^2/dr^2-l(l+1)/r^2-\gamma^2]H_l(r)=0$$

and

$$H_l(c)=\mathcal{J}_l(kc).$$

Since in our pure hard core, $v=0$ for $r>c$, we have

$$\int_c^\infty\chi_l(k_0r)\mathcal{J}_l(kr)dr=(k^2+\gamma^2)^{-1}\mathcal{J}_l(k_0c)[\mathcal{J}_l'(kc)-H_l'(c)].$$

It is interesting to note that in the above equation it is the term involving k_0 that remains undifferentiated, while the terms involving the final state k are differentiated with respect to r; whereas $\zeta_0(k_0)$ is the wave function that is distorted by the potential and not $\phi(k)$. From the Hermitian properties of the G matrix, it can be seen that a similar result can be derived for $\langle\mathbf{k}_0|G|\mathbf{k}\rangle$, where the roles of k and k_0 are interchanged. The value of γ for this expression will, however, be different so as to produce the same matrix element.

Equation (5) now becomes

$$\int_{r>c}\phi\zeta_0d\tau=(k^2+\gamma^2)^{-1}(kk_0)^{-1}$$
$$\times4\pi\textstyle\sum_l(2l+1)P_l(\hat{k}\cdot\hat{k}_0)\mathcal{J}_l(k_0c)[\mathcal{J}_l'(kc)-H_l'(c)].$$

Using

$$H_l'=\mathcal{J}_l(kc)[(d/dr)\ln H_l]_c$$
$$\simeq-\gamma[1+l(l+1)/2\gamma^2c^2]\mathcal{J}_l(kc),\qquad(7)$$

and the differential equation for $\mathcal{J}_l$ to eliminate $l(l+1)\mathcal{J}_l$, it can be shown that

$$\int_{r>c}\phi\zeta_0d\tau=4\pi c(k^2+\gamma^2)^{-1}\textstyle\sum_l(2l+1)P_l(\hat{k}.\hat{k}_0)j_l(k_0c)$$
$$\times\Big[j_l(kc)(1+\gamma c+k^2c/2\gamma)$$
$$+j_l'(kc)\Big(c+\frac{1}{\gamma}\Big)+\frac{c}{2\gamma}j_l''(kc)\Big]\qquad(8)$$

where

$$\mathcal{J}_l(x)=xj_l(x).$$

The sums over l can be evaluated in closed form using the identities

$$4\pi\textstyle\sum_l(2l+1)P_l(\hat{k}\cdot\hat{k}_0)j_l(kr)j_l(k_0r)=\int e^{-i\mathbf{q}\cdot\mathbf{r}}d\Omega$$
$$=4\pi j_0(qr),\qquad(9a)$$
$$4\pi\textstyle\sum_l(2l+1)P_l(\hat{k}\cdot\hat{k}_0)j_l'(kr)j_l(k_0r)$$
$$=-ik\int(\hat{k}\cdot\hat{r})e^{-i\mathbf{q}\cdot\mathbf{r}}d\Omega$$
$$=-ik\int P_1(\hat{k}\cdot\hat{q})P_1(\hat{q}\cdot\hat{r})e^{-i\mathbf{q}\cdot\mathbf{r}}d\Omega$$
$$=-4\pi kP_1(\hat{k}\cdot\hat{q})j_1(qr),\qquad(9b)$$

and

$$4\pi\textstyle\sum_l(2l+1)P_l(\hat{k}\cdot\hat{k}_0)j_l''(kr)j_l(k_0r)$$
$$=-k^2\int(\hat{k}\cdot\hat{r})^2e^{-i\mathbf{q}\cdot\mathbf{r}}d\Omega$$
$$=-k^2\int\frac{2P_2(\hat{k}\cdot r)+P_0(\hat{k}\cdot\hat{r})}{3}e^{-i\mathbf{q}\cdot\mathbf{r}}d\Omega$$
$$=4\pi k^2[\tfrac{2}{3}P_2(\hat{k}\cdot\hat{q})j_2(qr)-\tfrac{1}{3}P_0(\hat{k}\cdot\hat{q})j_0(qr)].\qquad(9c)$$

Putting (9a), (9b), and (9c) into Eq. (8), and adding to Eq. (4), we get

$$\langle\mathbf{k}|G|\mathbf{k}_0\rangle=4\pi(m^*)^{-1}\{(k^2+\gamma^2)[(qc)^2/q^3]j_1(qc)$$
$$+(c+\gamma c^2+k^2c^2/2\gamma)j_0(qc)$$
$$-(kc^2+kc/\gamma)j_1(qc)P_1(\hat{k}\cdot\hat{q})$$
$$+(k^2c^2/2\gamma)[\tfrac{2}{3}P_2(\hat{k}\cdot\hat{q})j_2(qc)-\tfrac{1}{3}j_0(qc)]\}.\qquad(10)$$

The above expression, though somewhat unhygienic in appearance, is nevertheless quite general, valid for all $\mathbf{k}$, $\mathbf{k}_0$, and any amount by which the interaction may be off the energy shell, provided one uses the reference spectrum. Besides, it reduces to simpler forms for the particular cases we have in mind.

III. THIRD-ORDER DIAGRAMS

We shall now discuss the third-order diagrams in detail, referring to Figs. 1(a)–1(h).

Fig. 1(b). This, along with its exchange in Fig. 1(c), is used by BBP to define their energy spectrum. The middle G_2 matrix is diagonal here, and can be obtained as a special case from Eq. (10) by putting $\mathbf{k}_0\rightarrow\mathbf{k}$. We then get

$$\langle\mathbf{k}|G|\mathbf{k}_0\rangle$$
$$=(m^*)^{-1}[(k^2+\gamma^2)V_c+4\pi c(1+\gamma c+k^2c/3\gamma)],\qquad(11)$$

where V_c= core volume. This is the result obtained by BBP for a hard core. Before this can be placed as an insert into the energy of particle b, it has to be summed over n and averaged over m and l. The resulting

contribution $U_2(b)$ to the energy of the particle b is

$$U_2(b)=\rho(m^*)^{-1}[\langle k^2+\gamma^2\rangle_{\rm av}V_c+4\pi c\langle 1+\gamma c+k^2c/3\gamma\rangle_{\rm av}],$$

where ρ=density of nuclear matter, $\mathbf{k}=\frac{1}{2}(\mathbf{b}-\mathbf{n})$ averaged over $\mathbf{n}$, $\gamma^2=\langle e-k^2/m^*\rangle_{\rm av}$, and e=excitation energy of the diagram.

Fig. 1(d). This diagram and those following it are those we are concerned with. They were in the past considered unimportant as compared to the bubble diagram. We will now proceed to show that they are comparable to the bubble diagram in Fig. 1(b), and consequently should and can be added as insertions into the single-particle energy of state b. The fact that Figs. 1(b) and 1(d) should be comparable can be seen from the simple argument that the momentum transfer involved in G_2 of Fig. 1(d) is $\mathbf{q}=\mathbf{m}-\mathbf{n}$. Since $\mathbf{m}$ and $\mathbf{n}$ are both inside the Fermi sea, q is on the average much smaller than $k_0=\frac{1}{2}|(\mathbf{a}-\mathbf{n})|$ or $k=\frac{1}{2}|(\mathbf{b}-\mathbf{m})|$, $\mathbf{a}$ and $\mathbf{b}$ being above the sea. Thus, for most values of b, the G_2 interaction of Fig. 1(d) is almost diagonal, and, therefore, there should not be much difference between Fig. 1(d) and Fig. 1(b).

The algebra gives the same result. Equation (10) for $\langle\mathbf{k}|G|\mathbf{k}_0\rangle$ reduces in this case to

$$\langle\mathbf{k}|G|\mathbf{k}_0\rangle=(m^*)^{-1}(k^2+\gamma^2)V_c[1-(qc)^2/10+\cdots]$$
$$+4\pi c(m^*)^{-1}(1+\gamma c+k^2c/3\gamma)[1-(qc)^2/6+\cdots].$$

In the above equation, we have averaged over the directions of $\mathbf{q}$ relative to $\mathbf{k}$. For nuclear matter, we have

$$\langle q^2\rangle=\langle m^2+n^2-2\mathbf{m}\cdot\mathbf{n}\rangle=\langle m^2\rangle+\langle n^2\rangle=1.2k_F^2,$$
$$c=0.4\text{ F},\quad k_F=1.5\text{ F}^{-1};$$

therefore

$$\langle q^2\rangle c^2\sim 0.432.$$

For Fig. 1(d), then,

$$\langle\mathbf{k}|G_2|\mathbf{k}_0\rangle=(m^*)^{-1}(k^2+\gamma^2)V_c(1-0.043+\cdots)$$
$$+4\pi c(m^*)^{-1}(1+\gamma c+k^2c/3\gamma)(1-0.072+\cdots).$$

Comparing this with Eq. (11) we can see that the two expressions are roughly of the same magnitude.

We can average the above expression over $\mathbf{m}$ and $\mathbf{l}$ and integrate over states $\mathbf{n}$, to obtain a contribution $U_4(b)$ to the single-particle energy, given by

$$U_4(b)=-\rho(m^*)^{-1}[0.96\langle k^2+\gamma^2\rangle_{\rm av}V_c$$
$$+(0.93)4\pi c\langle 1+\gamma c+k^2c/3\gamma\rangle_{\rm av}]. \quad (12)$$

The minus sign in front of ρ arises because of the sign convention used in the Goldstone method, in dealing with the different diagrams.[1]

Thus, we see that Fig. 1(d) can also be used as a self-energy insertion into $U(b)$, and its contribution $U_4(b)$ is comparable to $U_2(b)$ arising from Fig. 1(b).

Fig. 1(f). This diagram is similar to Fig. 1(d), inasmuch as it also has a particle-hole interaction in the middle. The contribution arising from this figure to $U(b)$ is, on the average equal to that from Fig. 1(d), and is hence given by Eq. (12).

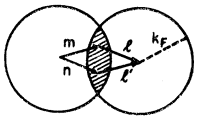

FIG. 2. Vector diagram in momentum space for the hole-hole interaction. The hole $\mathbf{n}$ is restricted to be in the shaded region.

Fig. 1(h). This is the "hole-hole" interaction which does not seem to directly involve the particle b. However, the value of γ^2 for this interaction will involve b and in fact has a term proportional to b^2 in it. Thus, this diagram can also be inserted in $U(b)$. The general expression (10) for $\langle\mathbf{k}|G|\mathbf{k}_0\rangle$ holds here as well, and can be shown to be of roughly the same order of magnitude, as in the previous cases.

The effect of this diagram, however, is considerably lessened by the following factors:

(i) The hole $\mathbf{n}$, for a given $\mathbf{m}$ and $\mathbf{l}$, cannot just be anywhere in the Fermi sea. It has to be such that the hole $\mathbf{l}'=\mathbf{m}+\mathbf{l}-\mathbf{n}$ is also inside the sea.

In the example shown (Fig. 2), $\mathbf{n}$ has to be inside the shaded region. It can be shown that on the average $\mathbf{n}$ traverses a quarter of the Fermi sphere. This multiplies the contribution of this diagram by a factor of 1/4.

(ii) Since the two nucleon loops are identical, one-half of the hole-hole interaction is associated with particle b and the other half with particle c. This introduces another factor of 1/2 on the contribution to $U(b)$.

Owing to these reasons, this diagram is relatively unimportant, but its effect, when necessary, can be calculated using expression (10) as before.

Figs. 1(c), 1(e), and 1(g). These are the only other diagrams in column A. They all have the common characteristic that their middle interaction converts states above the sea into those below the sea, and consequently involves a large momentum transfer. Using arguments similar to the ones used before, we can see that they will be roughly equal to each other. Fig. 1(c), which is the simplest, has

$$\mathbf{k}=\tfrac{1}{2}(\mathbf{b}-\mathbf{n}),\quad \mathbf{k}_0=\tfrac{1}{2}(\mathbf{n}-\mathbf{b})=-\mathbf{k};$$

therefore

$$\mathbf{q}=2\mathbf{k}\quad\text{and}\quad(\hat{q}\cdot\hat{k})=1.$$

Expression (10) then gives

$$\langle\mathbf{k}|G_2|-\mathbf{k}\rangle$$
$$=4\pi(m^*)^{-1}\Big[(k^2+\gamma^2)(\sin 2kc/8k^3-c\cos 2kc/4k^2)$$
$$+\frac{c\sin 2kc}{2kc}\left(\frac{1}{2}+\gamma c+\frac{1}{-4\gamma c}\right)$$
$$+c\cos 2kc\left(\frac{1}{2}+\frac{1}{4\gamma c}\right)\Big]. \quad (13)$$

Figures 1(e) and 1(g) will give roughly the same result since they have approximately the same γ, $\mathbf{k}$, and $\mathbf{q}$.

It should be noted here, for future use, that for large values of b, (13) is small compared to (11), and these diagrams do not influence $U(b)$ very much. However, for $b\sim 4$ F^{-1}, which is used as a typical value by BBP, (13) is about 4/7 of (11), thereby raising the relative importance of these diagrams to $U(b)$.

We have thus studied briefly, the contributions arising from all the diagrams in column A.

IV. RELATIVE WEIGHTS OF THE DIAGRAMS

If one uses a spin-independent potential, the different diagrams do not have the same weight. This is because a nucleon with a certain charge and spin component will not change these properties due to such an interaction. Thus, for example, in Fig. 1(d), once the hole **m** is defined, the hole **n** is forced to have the same z component of spin and isospin. Therefore, only 1/4 of the states inside the Fermi sea are allowed for **n**. Now, if in $U_4(b)$, we mean by ρ the actual density of nuclear matter regardless of spin or isospin, then we have to multiply the contribution by a factor of 1/4. The hole **n** in Fig. 1(b), however, can take all spin and charge states regardless of **m**, so that $U_2(b)$ should not be multiplied by 1/4.

As a general rule, it can be seen that all nucleons in a single "loop" must have the same charge and z component of spin. The relative weight of a diagram is hence given by $(1/4)^{\mu-\nu}$, where μ=number of independent states and ν=number of loops. The sign associated with each diagram[1] is given by $(-1)^{h+\nu}$, where h is the number of internal hole lines. The weights thus obtained, along with the appropriate signs, are given alongside the figures in both columns A and B.

V. CONCLUSION

The above considerations indicate that the single-particle potential energy of the state labelled "b" should be obtained by adding the averaged middle interaction from the diagrams 1(b) to 1(h), with the proper relative weights. This would essentially incorporate their effect into the first order diagram. Figure 3 shows the requirement on $U(b)$. Repeated use of Eq. (10) for all the cases in Fig. 3 gives $U(b)$ in detail. By choosing $U(b)$ thus, we can cancel Fig. 1(a) with all the other graphs of column A. It can be easily seen that the *same* choice of $U(b)$ also cancels Fig. 1(a′) with all other graphs of column B.

To estimate the effect of our procedure we note that the diagrams 1(b), (d), and (f) have in common that the momentum is changed only slightly [or, in (b), not at all] by the middle interaction. We have shown in Sec. II and III that the value of the matrix element is not much affected by the slight change of momentum. Therefore diagrams 1(b), (d), and (f) are approximately equal, apart from the statistical weight factor, and their sum is then just one-half of diagram 1(b). (The corrections to this statement can be calculated from Sec. II.) Similarly, diagrams 1(c), 1(e), and 1(g) all involve a large momentum change in the middle interaction approximately from a to m, and these momentum changes are again about equal; thus the sum of these diagrams (with statistical weights) is again one-half of the cluster diagram 1(e). Thus we find that the bubble interaction 1(b) should be replaced by

$$U\approx\tfrac{1}{2}[1(b)]+\tfrac{1}{2}[1(e)]. \quad (14)$$

It can be shown that, if the number of available spin-isospin states were n rather than 4, the factor $\frac{1}{2}$ in (14) would be replaced by $1-2/n$. In particular, for a pure neutron gas, this is zero.

Now the middle interaction in 1(b) is a "direct" interaction of particles n and b while 1(c) is an exchange interaction between these particles, and 1(e) is essentially the same. But the direct interaction may be written as the sum over the even plus a sum over the odd angular momenta, while the exchange interaction is even minus odd. Thus the effective total interaction, $1(b)$ to $1(g)$, is

$$U=\tfrac{1}{2}\text{ (direct)}+\tfrac{1}{2}\text{ (exchange)}=\text{(even } L\text{ only)}. \quad (15)$$

BBP, using only 1(b) and 1(c), get instead

$$U_{\text{BBP}}=\text{direct}-\tfrac{1}{4}\text{ (exchange)}$$
$$=\tfrac{3}{4}\text{ (even } L)+(5/4)\text{ (odd } L). \quad (16)$$

Similar conclusions can be drawn about the diagrams in column B. The diagram 1(h) has been omitted because of its small coefficient; it would add 0.03 times the direct term.

Our considerations are only valid for spin-independent, isotropic interactions. It has been shown by Bethe and Brandow[6] that the result is very similar if the forces are spin dependent but still isotropic. Tensor forces seem to give a somewhat different result.

To see the effect on the reference spectrum parameters, we note first that for large values of b, the matrix elements of the middle interaction for even and odd L are about equal (BBP Sec. 5). This is perhaps most evident if we remember that the exchange interaction 1(c) goes to zero in this limit. Therefore, for large b, the potential of BBP should be essentially reduced to half. For small b, on the other hand, the contribution from odd L is small, and if it is neglected, (15) is even bigger than (16). We do not believe that this result is significant because (a) even for k_b as small as k_F, the odd L are not negligible, and (b) tensor forces are important in the initial interaction leading from m to a state of low b, and for these (15) is not valid.

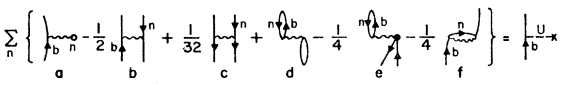

FIG. 3. The choice of single-particle energies.

[6] H. A. Bethe and B. H. Brandow (private ommunication).

We expect then that at small b the potential $U(b)$ will not be greatly changed from the result of BBP. Since it will be halved at large b, we believe that the effective mass correction, $1-m^*$, will be roughly divided by 2 while the constant term A_2 in the potential (7.1) of BBP will not be changed much. Detailed calculations are needed for more accurate predictions.

The only other third order graph that has not been considered here involves a hole-bubble interaction. This can, however, be absorbed in the hole energy as shown by BBP. Thus, all third-order diagrams are eliminated by this procedure which renders the first-order estimation for the binding energy correct up to third order.

Finally, it is clear that the above procedure not only eliminates all third-order graphs but also greatly reduces the effect of a very large number of fourth- and higher-order graphs that involve interactions shown in Fig. 3. The evaluation of the off-diagonal $\langle k|G|k_0\rangle$ also paves the way towards estimating the contribution of the remaining higher-order graphs which are not thus eliminated. Hopefully, they will not make large corrections to the binding energy.

ACKNOWLEDGMENTS

The author is greatly indebted to Professor H. A. Bethe for patiently initiating him into the problem of nuclear matter and for his constant advice and encouragement. He would also like to express his deep gratitude to B. H. Brandow and B. D. Day for many valuable clarifications and criticisms.

PHYSICAL REVIEW VOLUME 129, NUMBER 1 1 JANUARY 1963

New Isotope In^{122}

J. KANTELE* AND M. KARRAS
Department of Chemistry, University of Arkansas, Fayetteville, Arkansas†
(Received 23 July 1962)

A new isotope, In^{122}, has been produced by 14–15 MeV neutron bombardment of tin. The basis for mass and atomic number assignment is presented, as well as the following decay characteristics: half-life, 7.5±0.8 sec; beta end-point energy, 4.5±0.8 MeV; two coincident gamma rays having energies 1.140±0.010 MeV and 0.995±0.010 MeV.

IN connection with a systematic study[1] of the level structure of even tin isotopes resulting from the decay of neutron-excess indium isotopes, a new 7.5-sec activity was found and was assigned to the hitherto unknown isotope In^{122}. The purpose of this note is to report the principal decay characteristics of this new activity and the basis for assigning it to In^{122}.

In this investigation, the activity mentioned was produced upon irradiations of a 90.8% enriched metallic Sn^{122} sample with 14–15 MeV neutrons from the University of Arkansas 400-kV Cockcroft-Walton accelerator. Neither bombardments of highly enriched Sn^{118} (96.6%), Sn^{120} (98.39%), and Sn^{124} (96.0%) samples nor irradiations of natural tin produced any observable amount of the activity under consideration, due in the latter case to masking by other strong activities produced. In most experiments, the samples were sealed in light polyethylene ("Marlex") capsules that could be transported from the accelerator target to the spectroscopy laboratory in less than 0.5 sec with the aid of a pneumatic transport system. The radiations produced in the capsule itself [mainly radiations characteristic of N^{16} decay[3])] were studied and taken into account in analysis of the actual data. About 30 to 50 short runs were needed for acceptable statistics in most cases.

Gamma and beta radiations were investigated by means of scintillation detectors; namely, two 3 ×3-in. NaI(Tl) crystals for gamma-ray studies and a 1½-in. diam by 1-in. deep plastic crystal for rough beta spectroscopy. The sum-peak spectrometer[4] of our laboratory was also used for gamma-gamma coincidence studies. Due to low activities produced, resolving times of 0.4 to 0.9 μsec could be used, which assured complete electronic coincidence efficiency. Decay curves were obtained usually by using an RIDL 200-channel analyser as a multi-channel scaler.

Since the first (probably 2^+) excited state of Sn^{122} was known[5,6] to lie at 1.14 MeV, possible short-lived isomers of In^{122} could be expected to decay at least in

* Present address: Institute of Physics, University of Helsinki, Helsinki, Finland.
† Work supported in part by the U. S. Atomic Energy Commission.
[1] J. Kantele, M. Karras, and R. B. Moler (to be published).
[2] Supplied by the Isotopes Sales Department, Union Carbide Nuclear Company, Oak Ridge National Laboratory, Oak Ridge, Tennessee.
[3] *Nuclear Data Sheets* (Printing and Publishing Office, National Academy of Sciences–National Research Council, Washington 25, D. C.).
[4] J. Kantele and R. W. Fink, Nucl. Instr. Methods **15**, 69 (1962); J. Kantele, *ibid.* **17**, 33 (1962).
[5] D. G. Alkhazov, D. S. Andreev, K. I. Erokhina, and I. Kh. Lemberg, Zh. Eksperim. i. Teor. Fiz. **33**, 1347 (1957); [translation: Soviet Phys.—JETP **6**, 1036 (1958)].
[6] P. H. Stelson and F. K. McGowan, Phys. Rev. **110** 489 (1958).